Global Change Biology (2008) **14**, 757–767, doi: 10.1111/j.1365-2486.2008.01538.x

Calibration of Terra/MODIS gross primary production over an irrigated cropland on the North China Plain and an alpine meadow on the Tibetan Plateau

YONGQIANG ZHANG*, QIANG YU†, JIE JIANG† and YANHONG TANG‡
*CSIRO Land and Water, PO Box 1666, Canberra, ACT 2601, Australia, †Institute of Geographic Sciences and Natural Resources Research, Beijing 100101, China, ‡National Institute of Environmental Studies, Onogawa 16-2, Tsukuba 305-8506, Japan

Abstract

This paper evaluated the MODerate resolution Imaging Spectroradiometer (MODIS) gross primary production (GPP) product (MOD17) by using estimated GPP from eddy-covariance flux measurements over an irrigated winter wheat and maize double-cropping field on the North China Plain in 2003–2004, and an alpine meadow on the Tibetan Plateau in 2002–2003. The mean annual GPP from MOD17 accounted for 1/2–2/3 of the surface estimated mean annual GPP for the alpine meadow, but only about 1/5–1/3 for the cropland. This underestimation was partly attributed to low estimates of leaf area index by a MODIS product (MOD15) because it is used to calculate absorbed photosynthetically active radiation in the MOD17 algorithm. The main reason is that the parameter maximum light use efficiency (ε_{max}) in the MOD17 algorithm was underestimated for the two biomes, especially for the cropland. Contrasted to the default, ε_{max} was optimized using surface measurements. The optimized ε_{max} for winter wheat, maize and meadow was 1.18, 1.81 and 0.73 g C/MJ, respectively. By using the surface measurements and optimized ε_{max}, the MOD17 algorithm significantly improved the accuracy of GPP estimates. The optimum MOD17 algorithm explained about 82%, 68%, and 79% of GPP variance for winter wheat, maize, and meadow, respectively. These results suggest that it is necessary to adjust the MOD17 parameters for the estimation of cropland and meadow GPP, particularly over cropland.

Keywords: carbon dynamic, cropland, ecosystem respiration, eddy-covariance, gross primary production, meadow, MODIS

Received 26 July 2006; revised version received 12 September 2007 and accepted 12 October 2007

Introduction

There are over 240 flux stations globally (FLUXNET, http://www.daac.ornl.gov/FLUXNET/). These stations were established to measure fluxes of CO_2, water vapor and energy, and to estimate gross primary production (GPP), net primary production (NPP), and light use efficiency (LUE) in different biomes (Falge *et al*., 2002a, b; Law *et al*., 2002; Gu *et al*., 2003; Kato *et al*., 2004a; Lagergren *et al*., 2005; Leuning *et al*., 2005; Turner *et al*., 2005). Flux measurements at the stations provide a unique opportunity for understanding carbon cycle processes from hourly to yearly time scales, and for informing and parameterizing soil–vegetation–atmosphere models (Running *et al*., 1999; Baldocchi *et al*., 2001). Globally, flux-measured biomes across different climate zones, from tropical to frigid, include forests, grassland, crops and tundra (Falge *et al*., 2002a; Law *et al*., 2002). Such measurements make global validation of remotely sensed GPP and NPP possible.

In China, dozens of flux towers have also been placed in different biomes, including forests, grasslands and crops. Some of the towers belong to the ChinaFLUX network (www.chinaflux.net). These widely distributed biomes represent China's main ecosystems, and flux measurements at these biomes are used to estimate magnitude and temporal variation of GPP/NPP (Yu *et al*., 2006). Because China is among the largest countries in the Eurasian continent, covering almost all the climatic zones from tropical to frigid, CO_2 flux measurements and estimates of GPP/NPP over China's ecosys-

Correspondence: Yongqiang Zhang, tel. + 61 2 62465761, fax + 61 2 62465800, e-mail: yongqiang.zhang@csiro.au

tems will be helpful to improve the accuracy of the carbon budget in the North Hemisphere terrestrial ecosystems.

The alpine meadow and cropland play an important role in the regional carbon budget because of their large area in China (Zhang *et al*., 2002; Gu *et al*., 2003). The alpine meadow in China is widely distributed in high-elevation regions, and has been estimated to cover about 1/4 of the area of the Qinghai–Tibetan Plateau that extends to about 2.5 million km^2 (DAHV & GSAHV, 1996). The carbon density is very high in this biome and is estimated to be 40.4 $g\,C\,m^{-2}\,yr^{-1}$ of average aboveground carbon and 74.6 $g\,C\,m^{-2}\,yr^{-1}$ of belowground carbon for the alpine meadow biome over the plateau (Zhang *et al*., 2007). CO_2 flux measurements indicate that the alpine meadow currently behaves as a CO_2 sink (Kato *et al*., 2004a, b, 2006). The cropland biome covers the third largest area in China after grassland and forest biomes. The total area of cropland was 1.41 million km^2 in 2000, which is about 15% of the total land area of China (Liu *et al*., 2005). Cropland is regarded as a huge terrestrial carbon sink in China (Fang *et al*., 2007).

In a consistent manner, the global terrestrial GPP and NPP were monitored using data from the MODerate resolution Imaging Spectroradiometer (MODIS) sensor, aboard the US National Aeronautics and Space Administration (NASA) Terra satellite (Running *et al*., 2000, 2004). The MODIS NPP/GPP products called MOD17 are estimated by a simple light use efficiency algorithm for scientific research (Running *et al*., 2000). However, to have confidence in the MODIS NPP/GPP products, it is necessary to validate them against surface measurements. Several studies have been conducted to evaluate the MOD17 GPP product by using flux-tower measurements (Turner *et al*., 2003, 2005; Leuning *et al*., 2005). The MOD17 products seem to moderately underestimate NPP/GPP at an agricultural field site while strongly over-estimating NPP/GPP at desert grassland and dry coniferous forest sites. Very good estimates of NPP/GPP are at temperate deciduous forest, arctic tundra and boreal forest sites (Turner *et al*., 2005). The MOD17 products for a tropical savanna overestimate GPP in the dry season and low-rainfall summers, but give satisfactory results during wet seasons. When compared to flux-estimated GPP, MOD17 products give excellent estimates of the annual amplitude in GPP at a cool-temperature eucalyptus forest, but are less satisfactory in predicting seasonal variation (Leuning *et al*., 2005).

To contribute to global GPP research, the aims of this paper include (1) to evaluate the MOD17-GPP product by using flux measurements over the two biomes, an irrigated cropland and an alpine meadow and (2) to investigate potential ways to improve the quality of the MOD17-GPP product at the two biomes.

Methods

Site description

The two flux stations are Yucheng and Haibei in China. Table 1 gives a brief summary of vegetation, climate and soils at the two sites. The Yucheng flux station is located on the North China Plain. Land cover surrounding the station is an irrigated cropland of double-cropping winter wheat and summer maize, representing the main cropping system on the plain. Winter wheat is sown in early October and harvested in mid-June; summer maize is sown in mid-June and harvested in late September. Because rainfall is insufficient to support this double-cropping system, agricultural production around the station, particularly the production of winter wheat, depends upon surface ditch irrigation pumped from the Yellow River. The Haibei flux station is located on the northeastern Tibetan Plateau. Climate

Table 1 Site information for the cropland and alpine meadow sites

Site	Yucheng (cropland)		Haibei (alpine meadow)
Coordinates	116°34′13″E, 36°50′N		101°19′ 52″E, 37°39′55″N
Elevation (m)	28		3250
Climate	Warm temperature semihumid monsoon		Plateau-continental
Rainfall (mm)	582		580
Mean temperature (°C yr^{-1})	13.1		−1.7
Soils	Loam soil		High organic soil
Dominant species	Winter wheat	Summer maize	Three perennial sedges, *Kobresia humilis*, *Kobresia pygmaea* and *Kobresia tibetica* (Cyperaceae), and one dwarf shrub species, *Potentilla fruticosa* (Rosaceae)
Maximum canopy height (m)	1	3	0.3
Observation period	January–June 2003, October 2003–June 2004	July–September 2003 July–September 2004	January 2002–December 2003

in this area is characterized by low temperatures, high irradiance, low-atmospheric pressure, and relatively high precipitation. Land cover around the site is a C3-dominated alpine meadow. It starts to grow in May, and reaches maximum aboveground biomass and maximum leaf area index (LAI) during the period of July to August, when air temperature and precipitation are also at their peaks. The meadow then dries up and the shrubs become dormant in October.

Flux and LAI measurements

The water vapor and CO_2 fluxes were measured by an open-path eddy covariance system at Haibei station during the period 2001–2004. The system was set in the C3-*Kobresia* meadow with a fetch of atleast 250 m in all directions. The wind speed and sonic virtual temperature were measured at 2.2 m aboveground with a sonic anemometer (CSAT-3, Campbell Scientific Inc., Logan, UT, USA). CO_2 and water vapor concentrations were also measured at the same height with an open-path infrared gas analyzer (CS-7500, Campbell Scientific Inc.). Other ancillary measurements including micrometeorological variables, soil moisture and rainfall were simultaneously conducted at the same site. Fifteen-minute averages of all data were logged by an analog multiplexer (AM416, Campbell Scientific Inc.) and a digital micrologger (CR23X, Campbell Scientific Inc.) (Gu *et al*., 2003; Zhang & Tang, 2005).

The same kinds of eddy covariance system and ancillary measurement instruments were installed at the Yucheng station in November 2002. The eddy covariance system was installed at 2.1 m height aboveground during the winter wheat season and early maize growth period, and was elevated to 4.0 m aboveground when maize height was over 1.5 m. Thirty-minute averages of all data were logged by the digital micrologger (CR23X, Campbell Scientific Inc.) (Zhang & Tang, 2005; Zhang *et al*., 2005).

CO_2 and H_2O flux data at the two stations were processed with three common flux corrections, [i.e. three-dimensional rotation of coordinates, trend removal and sonic velocity correlation for water vapor density; (Gu *et al*., 2003; Kato *et al*., 2004b; Zhang *et al*., 2005; Wen *et al*., 2006)]. Correction was also made for reducing the effect of air density fluctuation on CO_2 and H_2O fluxes (Webb *et al*., 1980; Falge *et al*., 2002a). Daytime missing data were extrapolated from a 7-day moving window (Falge *et al*., 2001).

To estimate seasonal variation of surface fractional photosynthetically active radiation (FPAR) at Yucheng and Haibei stations, we used two sets of LAI data. The LAI measurements were taken on 7 separated days at Haibei station in 2002, but 57 separate days at Yucheng station in 2003–2004. In each measurement, five quadrats of 50 cm × 50 cm were randomly selected within the fetch area of flux tower. The average LAI from the five quadrats was taken as the site LAI at each measurement (Gu *et al*., 2003).

MOD15 and MOD17 products

To evaluate the MOD17-GPP product (GPP-MOD1) at the two sites, we downloaded the MOD15A2 and MOD17A2 products from the Land Processes-Distributed Active Archive Center (LPDAAC) (http://lpdaac.usgs.gov/dataproducts.asp). We selected the products from around the Haibei station for a 2-year period from January 1, 2002, to December 31, 2003, and around the Yucheng station for a 2-year period from January 1, 2003, to December 31, 2004. The MOD15 data product estimates 8-day composites of LAI and FPAR, whereas the MOD17 data product estimates 8-day composites of GPP and NPP. All the products are MODIS Collection 4 data at 1 km resolution and are an improved version of MODIS land science products. Each product of the MODIS data set includes data layers and Quality Assessment (QA) layers. MOD15 and MOD17 QA science data sets are in 8 bits, which determine data quality by using an index table (http://edcdaac.usgs.gov/modis/qa/moyd17a2_qa_v4.asp). All the MOD15 and MOD17 products with bad quality were rejected for further comparison with surface measurements (Zhang & Wegehenkel, 2006).

GPP calculations

Data of CO_2 flux [e.g. net ecosystem exchange, NEE ($mg\,CO_2\,m^{-2}\,s^{-1}$)] were summed to estimate daily GPP (GPP-FLUX) as

$$\mathrm{GPP} = -\sum \mathrm{NEE} + \sum R_e \text{ during daylight periods}, \quad (1)$$

where R_e is ecosystem respiration ($mg\,CO_2\,m^{-2}\,s^{-1}$). Negative values of NEE indicate a CO_2 sink, and conversely, positive values of NEE indicate a CO_2 source. It is difficult to measure daytime R_e directly. However, daytime R_e can be deduced from nocturnal NEE (assumed as nocturnal R_e), and soil temperature can be deduced using the simple Arrhenius function (Lloyd & Taylor, 1994). Fitting the modified Arrhenius equation to the nocturnal NEE data yielded:

$$R_e = R_{e,T_{ref}} \exp\left[(E_a/R)\left[\frac{1}{T_{ref}} - \frac{1}{T_s}\right]\right], \quad (2)$$

where $R_{e,T_{ref}}$ is the ecosystem respiration rate ($mg\,CO_2\,m^{-2}\,s^{-1}$) at the reference temperature T_{ref} (283.16 K), E_a is the activation energy ($J\,mol^{-1}$), R is a

gas constant ($8.134\,J\,K^{-1}\,mol^{-1}$) and T_s is the soil temperature at a depth of 5 cm. $R_{e,T_{ref}}$ and E_a are fitted parameters.

R_e was evaluated for each 2-month period, starting January 1, over the meadow site, and for each 3-month period, starting January 1, over the cropland. Nocturnal NEE and T_s data at strong turbulence (e.g. friction velocity was over a threshold $0.20\,m\,s^{-1}$) were selected to calibrate Eqn (2). Calibration was achieved by using the generalized pattern search algorithm, a widely used optimization method (Franchini *et al*., 1998).

The calibrated Arrhenius function during night-time periods was applied to extrapolate daytime R_e, and subsequently was used to calculate GPP according to Eqn (1). Daytime for calculating GPP was defined as periods when incoming solar radiation (S_t) was over $0.5\,W\,m^{-2}$ (Leuning *et al*., 2005). Daily GPP data were summed over an 8-day period, which was in accordance with the MOD17 GPP product period record.

The MOD17 algorithm

GPP in the MOD17 algorithm is calculated from light use efficiency (ε, $g\,C\,MJ^{-1}$) and absorbed photosynthetically active radiation (APAR, $MJ\,day^{-1}$) as

$$GPP = \varepsilon APAR. \tag{3}$$

APAR is derived from the measurements of PAR, which is calculated as 0.45 of solar radiation (S_t) multiplied by FPAR. FPAR is estimated from LAI by a simple Beer's Law approach (Jarvis & Leverenz, 1983):

$$FPAR = 1 - (e^{(LAI-K)}), \tag{4}$$

where K is the canopy light extinction coefficient. The K value for croplands and meadow is assumed to be 0.50, which is the same as the given value in the MOD17 algorithm and in Biome-BGC (Running *et al*., 2000; Turner *et al*., 2003, 2005).

The light use efficiency ε is calculated from the maximum ε (ε_{max}) and two functions, a function of vapor-pressured deficit (VPD) and a function minimum air temperature ($T_{a\,min}$). These two functions account for the effects of atmospheric humidity deficit and minimum temperature on carbon uptake according to the relationship:

$$\varepsilon = \varepsilon_{max} f(VPD) g(T_{a\,min}), \tag{5}$$

ε_{max} is assumed to be a constant for each biome in the MOD17 algorithm (Running *et al*., 2000). The functions of VPD and $T_{a\,min}$ in the MOD17 algorithm are given by

$$f(VPD) = \begin{cases} 0, & VPD > VPD_{max} \\ \frac{VPD_{max} - VPD}{VPD_{max} - VPD_{min}}, & VPD_{min} < VPD < VPD_{max} \\ 1, & VPD < VPD_{min} \end{cases} \tag{6}$$

and

$$g(T_{a\,min}) = \begin{cases} 0, & T_{a\,min} < T_{a\,min\_min} \\ \frac{T_{a\,min} - T_{a\,min\_min}}{T_{a\,min\_max} - T_{a\,min\_max}}, & T_{a\,min\_min} < T_{a\,min} < T_{a\,min\_max} \\ 1, & T_{a\,min} < T_{a\,min\_Tmax} \end{cases}. \tag{7}$$

To calculate GPP-MOD1, the FPAR in the MOD17 algorithm was taken from MOD15 products and PAR, VPD and $T_{a\,min}$ were acquired from NASA's Data Assimilation Office (DAO) climate data, which at the original coarse resolution were interpolated to the 1 km resolution (Heinsch *et al*., 2003). The default parameter values were used to calculate GPP-MOD1 for crops and grass (Table 2).

Using the same default parameter values and inputs of surface-measured PAR, VPD and $T_{a\,min}$ at these two sites, the MOD17 algorithm also calculated GPP, called GPP-MOD2.

Statistical analysis

The correspondence between simulated and surface-estimated values of R_e and GPP was analyzed using the index of agreement (IA) (Willmott, 1982) and the

Table 2 Values for ε_{max} ($g\,C\,MJ^{-1}$), $T_{a\,min\_max}$ (°C), $T_{a\,min\_min}$(°C), VPD_{max} (kPa), VPD_{min} (kPa) used for GPP calculation

Vegetation	ε_{max}	$T_{a\,min\_max}$	$T_{a\,min\_min}$	VPD_{max}	VPD_{min}	N	R^2
Mod17-crop	0.68	12.01	−8.0	4.1	0.65	–	–
Mod17-grass	0.68	12.01	−8.0	3.5	0.65	–	–
Winter wheat	1.18*	12.01	−8.0	4.1	0.65	360	0.82
Maize	1.81*	12.01	−8.0	4.1	0.65	204	0.68
Alpine meadow	0.73*	12.01	−8.0	3.5	0.65	485	0.79

*The parameter values with stars were optimized, whereas the parameter values without stars were default values in the MOD17 algorithm.

GPP, gross primary production; MOD17, MODerate resolution Imaging Spectroradiometer GPP product; VPD, vapor-pressured deficit.

root mean square error (RMSE), defined as

$$\mathrm{IA} = 1 - \frac{\sum_{j=1}^{N} (x_{\mathrm{sim}} - x_{\mathrm{obs}})_j^2}{\sum_{j=1}^{N} (|x_{\mathrm{sim}} - \bar{x}_{\mathrm{obs}}| + |x_{\mathrm{obs}} - \bar{x}_{\mathrm{obs}}|)_j^2} \quad (8)$$

$$\mathrm{RMSE} = \sqrt{\frac{\sum_{j=1}^{N} (x_{\mathrm{sim}} - x_{\mathrm{obs}})_j^2}{N-1}} \quad (9)$$

where x_{sim} and x_{obs} are the simulated and surface-estimated values and $\bar{x}_{\mathrm{obs}}$ is the arithmetic mean of the surface-estimated values, j is the jth sample, and N is the sample number. The IA ranges between 0 and 1, and the closer it is to 1, the better the correspondence is between surface-estimated and simulated outputs.

Results

The calibrated Arrhenius function

Figure 1 shows the changes of simulated and measured nocturnal R_e with the increase of T_s at the two biomes. The simulated R_e by the calibrated Arrhenius function corresponded sufficiently with that measured, indicated by an R^2 of 0.46, an IA of 0.77 and an RMSE $0.084\,\mathrm{mg\,CO_2\,m^{-2}\,s^{-1}}$ at Yucheng and an R^2 of 0.28, an IA of 0.60 and an RMSE of $0.13\,\mathrm{mg\,CO_2\,m^{-2}\,s^{-1}}$ at Haibei.

GPP comparisons

Figure 2 describes estimated GPP variation for the flux (GPP-FLUX), as well as GPP-MOD1 and GPP-MOD2 at the two sites. Strong seasonal variation of GPP was indicated by GPP-FLUX, GPP-MOD1 and GPP-MOD2 at both the sites. GPP-MOD1 agreed well with GPP-FLUX in the pregrowing seasons, but it was less than GPP-FLUX at both the sites in the growth seasons. The comparison of GPP-FLUX with GPP-MOD1 for the cropland obtained an IA of 0.50 and an RMSE of $5.95\,\mathrm{g\,C^{-2}\,day^{-1}}$ (Fig. 2a) in the growth season from March to November. The same comparison for the alpine meadow obtained an IA of 0.72 and an RMSE of $1.47\,\mathrm{g\,C^{-2}\,day^{-1}}$ (Fig. 2b) during the growth season from May to October. For both the biomes, GPP-MOD2 corresponded well with GPP-FLUX in the pregrowing seasons. GPP-MOD2 compared poorly with GPP-FLUX at the cropland in the growth seasons, with RMSE = $5.12\,\mathrm{g\,C^{-2}\,day^{-1}}$ and IA = 0.59. In contrast to that comparison, a better comparison of GPP-MOD2 with GPP-FLUX was found at the meadow in its growth seasons (RMSE = $1.86\,\mathrm{g\,C^{-2}\,day^{-1}}$ and IA = 0.67). In the same growth period, GPP for the cropland was much higher than that for the meadow.

GPP-MOD1 was further compared with GPP-MOD2 when the winter wheat (its season: October–mid-June) and maize (its season: July–September) were individually considered at the cropland (Fig. 3). For winter wheat, GPP-MOD2 compared poorly to GPP-MOD1 ($R^2 = 0.16$ and RMSE = $12.47\,\mathrm{g\,C\,m^{-2}}$) (Fig. 3c). The same comparison for maize showed a still lower R^2 of 0.20 and a high RMSE of $11.11\,\mathrm{g\,C\,m^{-2}}$ (Fig. 3b). GPP-MOD2 for the meadow was significantly lower than GPP-MOD1 with a slope of 0.53, an R^2 of 0.58 and an RMSE of $8.66\,\mathrm{g\,C\,m^{-2}}$ (Fig. 3c).

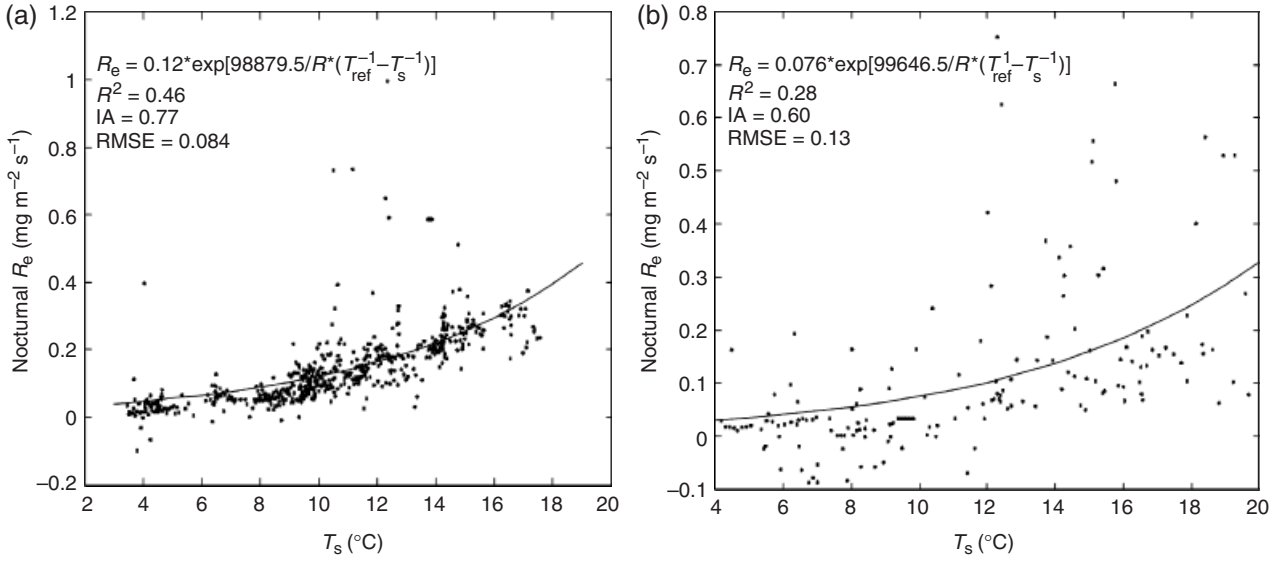

Fig. 1 Simulation of nocturnal ecosystem respiration (R_e) using the Arrhenius function at the Yucheng station (a) for the period April to June, 2004, and at the Haibei station (b) for the period May to July, 2002.

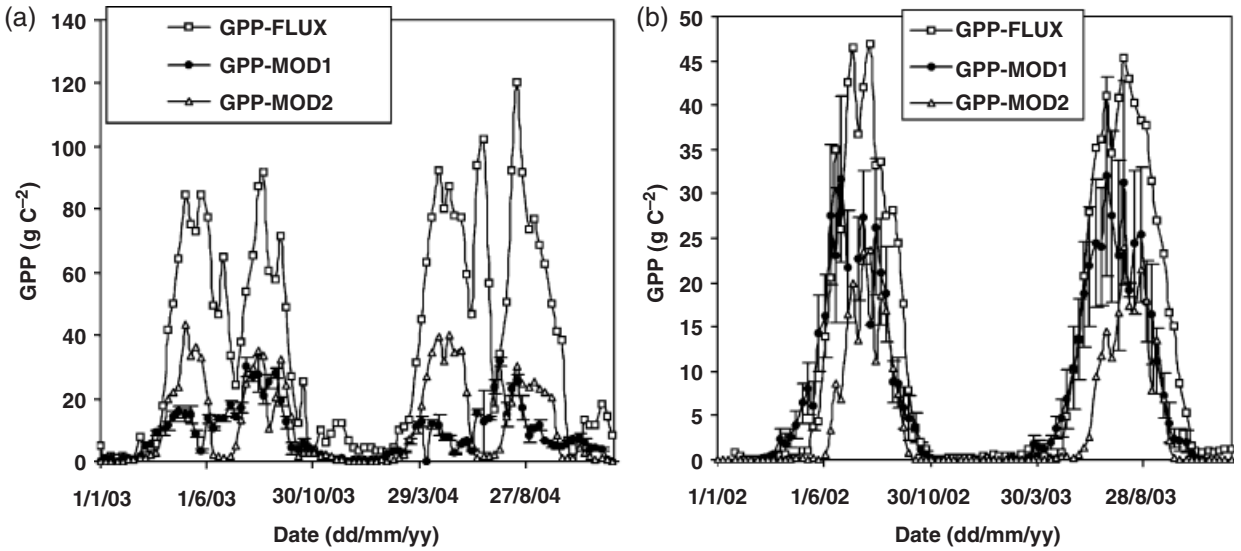

Fig. 2 Times series of 8-day gross primary production (GPP) estimated from the flux measurements, 8-day MOD17 GPP (GPP-MOD1) and 8-day GPP calculated from the MOD17 algorithm using the surface measurement inputs and default parameters (GPP-MOD2) at Yucheng (a) and Haibei (b). The error bar for GPP-MOD1 means that MOD17 GPP was averaged over 25 1-km^2 cells. Note that Kato *et al.* (2004b) first published the original net ecosystem exchange data at the Haibei station in 2002.

The annual comparison of the three types of GPP is listed in Table 3. Annual GPP-FLUX for the cropland was 1520 and 1958 g C m^{-2} yr^{-1} in 2003 and 2004, respectively, while annual GPP-MOD1 for the cropland was only about 1/5–1/3 of the annual GPP-FLUX. Annual GPP-MOD2 for the cropland was about 100–200 g C m^{-2} yr^{-1}, higher than the annual GPP-MOD1, but was only about 1/3 of the annual GPP-FLUX. Annual GPP-FLUX for the meadow was 504 and 605 g C m^{-2} yr^{-1} in 2002 and 2003, respectively. Annual GPP-MOD1 for the meadow was about 1/2–2/3 of the annual GPP-FLUX. Annual GPP-MOD2 for the meadow was about 100–200 g C m^{-2} yr^{-1}, lower than the annual GPP-MOD1, and it was only about 1/3 of the annual GPP-FLUX. Standard deviation of GPP-MOD1 at the cropland was 11% and 14% in 2003 and 2004, whereas that at the meadow was 31% and 39% in 2002 and 2003 (Table 3). This result indicates that the meadow exhibited a larger spatial heterogeneity in GPP than the cropland, although annual GPP-FLUX for the meadow was only about 1/3 of that for the cropland.

Figure 4 describes the strong seasonal dynamics of surface-estimated FPAR (FPAR-surf) and MOD15 FPAR (FPAR-MOD). FPAR-MOD was remarkably lower than FPAR-surf in the winter wheat growth seasons, with 58% underestimation of the average FPAR-surf; the average FPAR-MOD was also about 19% lower than the average FPAR-surf in the maize growth seasons. FPAR-MOD compared well with FPAR-surf in the period of June to September 2002, when LAI measurements were carried out.

ε_{max} optimization in the MOD17 algorithm

GPP-MOD1 and GPP-FLUX comparisons showed that the parameters in the MOD17 algorithm were erroneously estimated at the cropland and meadow. The peak values of GPP-MOD1 were highly dependent on ε_{max}, whose underestimation in Eqn (5) directly causes the underestimation of GPP. ε_{max} was optimized using the daily inputs of APAR, $T_{a\,min}$ and VPD, while other parameters were fixed (Table 2). The optimized ε_{max} values for winter wheat and maize were 1.18 and 1.81 g C MJ^{-1}, respectively, which are much larger than 0.68 g C MJ^{-1} fixed for crop in the MOD17 algorithm. The optimized ε_{max} value for the alpine meadow was 0.73 g C MJ^{-1}, compared to 0.68 g C MJ^{-1}, the MOD17 default value for grass.

Figure 5 shows the comparison between GPP-FLUX and the calculated GPP (GPP-MOD3) with the MOD17 algorithm, using surface measurements and optimized ε_{max}. For winter wheat, GPP-MOD3 compared well to GPP-FLUX, indicated by a linear regression slope of 0.90, an R^2 of 0.82, an IA of 0.95 and an RMSE of 1.69 g C m^{-2} day^{-1}. GPP-MOD3 for maize explained 68% variance ($R^2 = 0.68$) in GPP-FLUX, with a linear regression slope of 0.89, an IA of 0.90 and an RMSE of 2.81 g C m^{-2} day^{-1}. GPP-MOD3 for the alpine meadow compared well with the

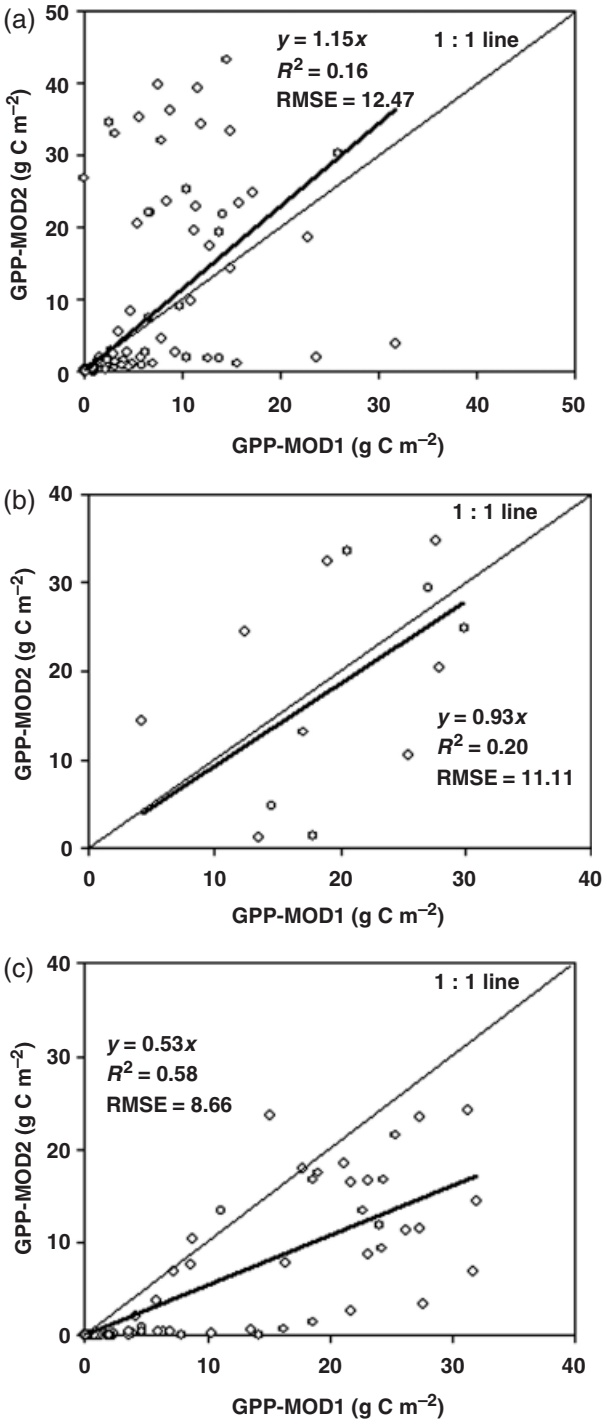

Fig. 3 Comparison of 8-day MOD17 gross primary production (GPP) (GPP-MOD1) and 8-day GPP calculated from the MOD17 algorithm using the surface measurement inputs and default parameters (GPP-MOD2) for winter wheat (a), maize (b) and meadow (c).

GPP-FLUX, and showed a linear slope of 0.87, an R^2 of 0.79, an IA of 0.94 and an RMSE of $0.96\,g\,C\,m^{-2}\,day^{-1}$.

Discussion

The uncertainty of GPP-FLUX estimates was mainly caused by errors in the estimation of R_e because the eddy-covariance technique is a standard method in monitoring ecosystem CO_2 exchange. In this study, R_e during daytime was estimated by the Arrhenius curve when it was calibrated using CO_2 flux measurements and 5-cm depth soil temperature during night-time. As shown in Fig. 1, the calibrated Arrhenius curve predicted night-time R_e with significant errors at the Haibei site. Another similar study at the Haibei site (Kato *et al*., 2004a, b) showed that R^2 between the measured and Arrhenius curve simulated R_e was <0.44 when the curve was calibrated in each month. Despite many errors in calculating R_e, the Arrhenius curve was considered very useful because R_e estimated from this method compared well with that calculated from the light response relationships (Falge *et al*., 2002a).

GPP-FLUX estimates for the meadow and cropland in this study were comparable with similar studies. Annual GPP-FLUX for the meadow in this study was slightly different from that estimated in another study (Kato *et al*., 2006). GPP-FLUX for the same meadow from their study was 575.1 and $647.3\,g\,C\,m^{-2}\,yr^{-1}$ in 2002 and 2003. This is compared to 503.9 and $604.7\,g\,C\,m^{-2}\,yr^{-1}$ in the same years, in the current study. The annual GPP-FLUX in this study was almost the same as $542\,g\,C\,m^{-2}\,yr^{-1}$ for a C3-grassland, remarkably lower than $1715\,g\,C\,m^{-2}\,yr^{-1}$ for a temperate C4-grassland (Falge *et al*., 2002a). The annual GPP-FLUX for the double-cropping cropland was clearly higher than that of other C3 wheat or soybean sites ($559–1396\,g\,C\,m^{-2}\,yr^{-1}$), and slightly higher than $1471\,g\,C\,m^{-2}\,yr^{-1}$ from a C4 maize site. It was also comparable to $1000–2000\,g\,C\,m^{-2}\,yr^{-1}$ from temperate coniferous forests (Falge *et al*., 2002a).

The underestimation of GPP-MOD1 at the two sites was caused by two types of errors: the errors in data inputs and the errors in the MOD17 GPP algorithm. The fact that FPAR-MOD was remarkably lower than FPAR-surf in winter wheat growth seasons, and sometimes lower than FPAR-surf in maize seasons (Fig. 4), suggests that MOD15 LAI at the cropland was significantly underestimated, resulting in an underestimation of APAR and GPP-MOD1. The errors in the MOD17 GPP algorithm were indicated by the GPP-MOD2, which was obviously less than the GPP-FLUX at the two sites. However, the seasonal trend in GPP-MOD2 was very similar to that in GPP-FLUX. The results hint that errors in $f(\mathrm{VPD})g(T_{a\,min})$APAR in the MOD17 algorithm were not significant. The main uncertainty of GPP-MOD1 was attributed to the underestimation of ε_{max} because GPP was well estimated using the optimized ε_{max} (Fig. 5),

Table 3 Annual GPP comparison among the estimates from flux measurement, the MOD17 product (GPP-MOD1) and the calculated (GPP-MOD2) from the MOD17 algorithm using surface measurement inputs

Site	Year	GPP (measured)	NPP (measured)	R_e (estimated)	GPP-MOD1	GPP-MOD2
Yucheng	2003	1520.2	761.2	759.0	437.3 (48.0)	512.7
	2004	1957.8	1097.3	860.5	371.8 (52.6)	545.6
Haibei	2002	503.9	263.8	240.1	313.4 (95.7)	186.2
	2003	604.7	394.7	210.0	332.0 (128.6)	197.5

Values in parentheses are standard deviations. Unit is $g\,C\,m^{-2}\,yr^{-1}$.
GPP, gross primary production; MOD17, MODerate resolution Imaging Spectroradiometer GPP product; NPP, net primary production; R_e, ecosystem respiration.

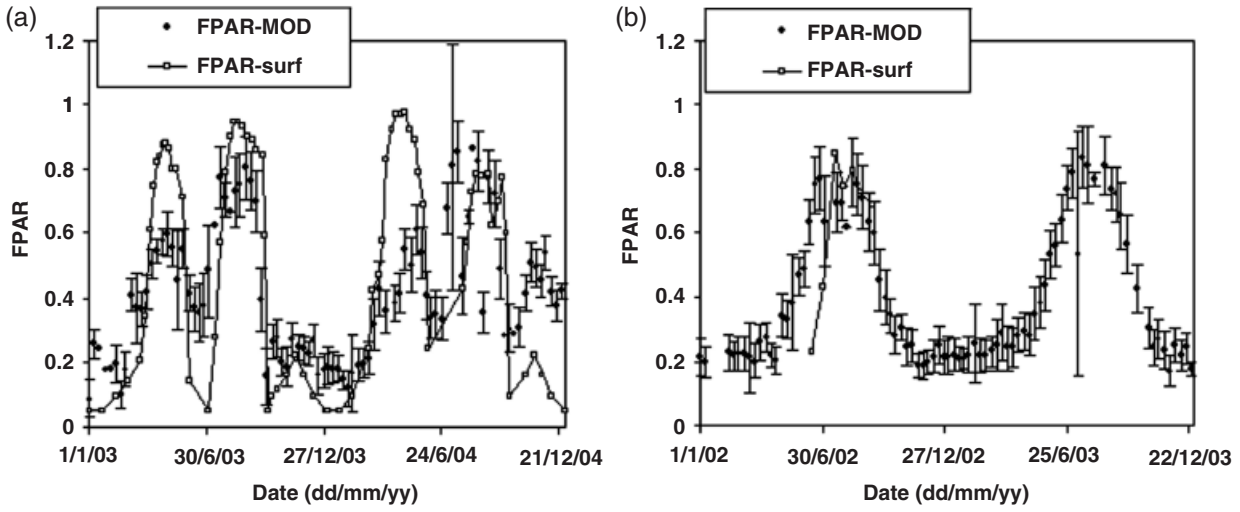

Fig. 4 Time series of surface-estimated fractional photosynthetic active radiation (FPAR) (FPAR-surf) and MOD15 FPAR (FPAR-mod) at Yucheng (a) and Haibei (b). The error bar for FPAR-mod means that MOD15 FPAR was averaged over 25 1-km^2 cells.

indicated by low RMSEs and slight deviation to the 1 : 1 line. It is necessary to calibrate the MOD17 algorithm at the two biomes, especially at the double-cropping field, which is one of the most extensive land cover types in the North China Plain.

Maize showed higher peak values of GPP-FLUX than winter wheat and meadow, which may suggest that light use efficiency was higher in C4 plants than C3 plants as observed in the winter wheat or the alpine meadow (Fig. 2). At the leaf level, C4 plants have a more efficient photosynthetic pathway than C3 plants. At the canopy scale, ε_{max} (Table 2) obtained in the current study indicates also a higher light use efficiency in C4 than C3 plants. This was perhaps mainly attributed to the very low temperature at the alpine meadow. Mean annual air temperature at Yucheng was 13.1 °C, contrasting to −1.7 °C at Haibei (Table 1). Contrary to our results, it was found that closed C_3 wheat assimilates CO_2 at a higher rate than a sparse C_4 maize canopy (Baldocchi, 1994). The lower GPP values in the sparse maize canopy may be caused by corn canopy's lower quantum yield, as it absorbs less PAR than the closed wheat stand (Baldocchi, 1994).

Soil water deficit was not a major factor influencing GPP at either site. Irrigation was applied at the Yucheng station when crops were under water deficit, and precipitation was enough to equal evapotranspiration at the Haibei station. The MOD17 algorithm did not include the impact of soil water availability on primary productivity. However, in semi-arid and arid regions where vegetation is not irrigated, soil water availability significantly influences GPP, as photosynthesis is closely coupled with water supply to the leaves from the soil via the roots, and with loss of water vapor from the leaves to the atmosphere (Leuning, 2004). Leuning *et al.* (2005) presented an index of soil moisture availability varying between 0 and 1 by using precipitation and APAR. The index was appended to the MOD17 algorithm after f(VPD) and $g(T_{a\,min})$. The revised algorithm estimated GPP at a semi-arid savanna, much better than the original MOD17 algorithm. Hence, to make the MOD17 algorithm more useful in semi-arid to arid

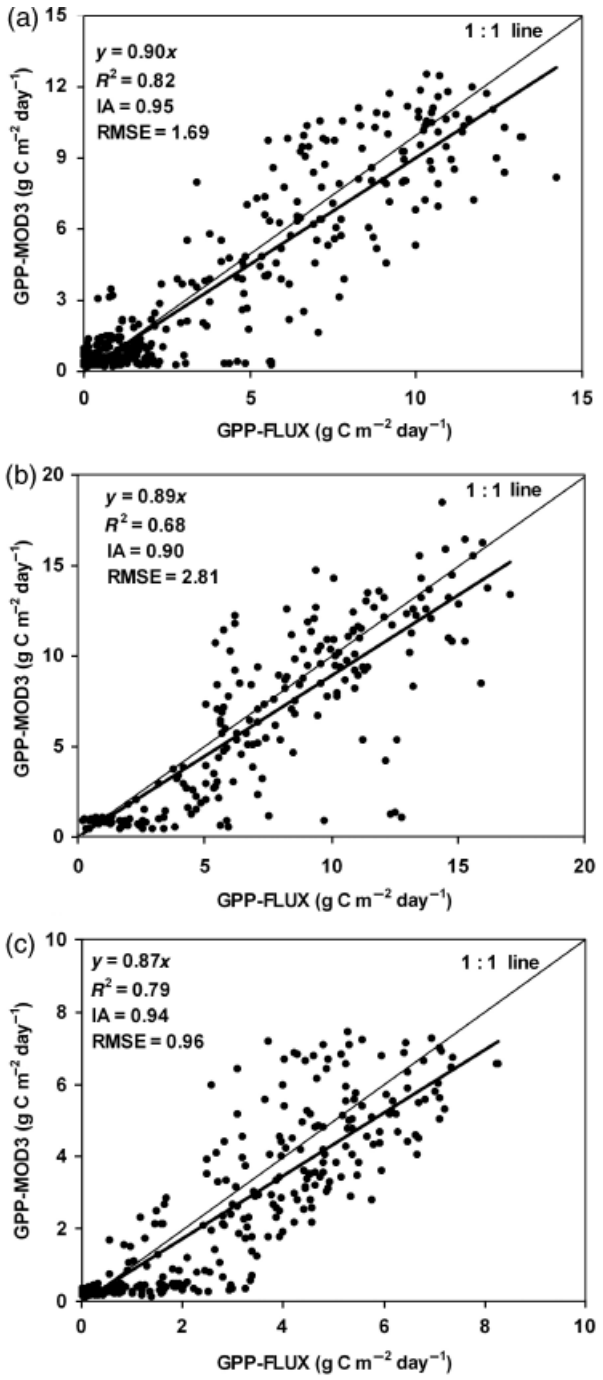

Fig. 5 Comparisons of the flux-measured GPP and calculated from the MOD17 algorithm by using the surface measurement inputs and optimized maximum light use efficiency in Table 2 (GPP-MOD3) for winter wheat (a), maize (b) and meadow (c).

regions, it is necessary to include a suitable soil water index in the algorithm.

The inaccuracy of the MOD17 products found at the two specific flux sites, especially for the cropland may provide some insights into its application for other flux sites in the world. There are 11 biomes defined in the MOD17 algorithm, including five types of forests, one type of woodland, two types of shrubland, two types of grasslands and one type of cropland (Heinsch *et al.*, 2003). This study suggests that MOD17 parameters for croplands should be revised and more types of croplands may be defined. Atleast 85 cropland flux stations belong to the global FLUXNET, which provide opportunities to re-define the MOD17 cropland parameters. The MOD17 algorithm only includes two grassland biomes: grasslands and wooded grassland. Obviously, for other specific grasslands, such as alpine meadow and wetlands, the algorithm needs to be calibrated because CO_2 flux measurements were widely carried out at these biomes (Aurela *et al.*, 2001; Gu *et al.*, 2003). The two sites in the current study are not spatially heterogeneous. A spatially heterogeneous biome (e.g. cropland/natural vegetation mosaic) may tend to result in a more inaccurate application of the MOD17. To obtain good quality of MOD17 GPP/NPP products, it is necessary to verify the MOD17 algorithm in different biomes, especially for those with strong human influences.

Conclusions

GPP estimates from the flux measurements over the alpine meadow and irrigated cropland are representative of major land cover types in the Tibetan Plateau and the North China Plain. The validation in this study indicates that the MOD17 GPP was underestimated at both the sites, particularly for the cropland. The results suggest that the parameter ε_{max} for the cropland in the MOD17 algorithm needs to be adjusted. Cropland with rotation such as the double-cropping field has not been considered so far as a land cover type in the MOD17 algorithm. Our results indicate that MOD17 does not seem to provide a correct estimation of GPP/NPP for a mixed-cropping or double-cropping system. Land use data with fine resolution should be combined with the MOD17 algorithm in order to improve the accuracy of the MOD17 products.

Acknowledgements

The first author is very grateful for his Alexander von Humboldt Fellowship in Germany. The study was supported by a special foundation by the Chinese Academy of Sciences (Grant No. O7R70020SD) and by a study on the effects of global warming on the Tibetan Plateau, funded by the MOE, Japan. We thank Drs Tomomichi Kato, Song Gu, Mingyun Du, Yinnian Li and Xinquan Zhao for their contributions in data collection and data processing at the Haibei station. We are grateful to anonymous reviewers and the editor for their critical reviews and construc-

tive suggestions. We extend our thanks to Dr Freddie Mpelasoka of CSIRO, Australia, for some corrections of this paper.

References

Aurela M, Lauria T, Tuovinen JP (2001) Seasonal CO_2 balances of a subarctic mire. *Journal of Geophysical Research – Atmospheres*, **106**, 1623–1637.

Baldocchi D (1994) A comparative-study of mass and energy-exchange rates over a closed C-3 (wheat) and an open C-4 (corn) crop. 2. CO_2 exchange and water-use efficiency. *Agricultural and Forest Meteorology*, **67**, 291–321.

Baldocchi D, Falge E, Gu LH *et al*. (2001) FLUXNET: a new tool to study the temporal and spatial variability of ecosystem-scale carbon dioxide, water vapor, and energy flux densities. *Bulletin of the American Meteorological Society*, **82**, 2415–2434.

DAHV (Department of Animal Husbandry and Veterinary) and GSAHV (General Station of Animal Husbandry and Veterinary) of Ministry of Agriculture of China (1996) *Rangeland Resources of China*. Chinese Science and Technology Press, Beijing (in Chinese).

Falge E, Baldocchi D, Olson R *et al*. (2001) Gap filling strategies for defensible annual sums of net ecosystem exchange. *Agricultural and Forest Meteorology*, **107**, 43–69.

Falge E, Baldocchi D, Tenhunen J *et al*. (2002a) Seasonality of ecosystem respiration and gross primary production as derived from FLUXNET measurements. *Agricultural and Forest Meteorology*, **113**, 53–74.

Falge E, Tenhunen J, Baldocchi D *et al*. (2002b) Phase and amplitude of ecosystem carbon release and uptake potentials as derived from FLUXNET measurements. *Agricultural and Forest Meteorology*, **113**, 75–95.

Fang JY, Guo ZD, Piao SL *et al*. (2007) Terrestrial vegetation carbon sinks in China, 1981–2000. *Science in China Series D: Earth Sciences*, **50**, 1341–1350.

Franchini M, Galeati G, Berra S (1998) Global optimization techniques for the calibration of conceptual rainfall-runoff models. *Hydrological Sciences Journal – Journal Des Sciences Hydrologiques*, **43**, 443–458.

Gu S, Tang YH, Du MY *et al*. (2003) Short-term variation of CO_2 flux in relation to environmental controls in an alpine meadow on the Qinghai–Tibetan Plateau. *Journal of Geophysical Research-Atmospheres*, **108**, 4670, doi: 4610.1029/2003JD03584.

Heinsch FA, Reeves M, Bower CF (2003) User's Guide, GPP and NPP (MOD17A2/A3) Products, NASA MODIS Land Algorithm, http://www.forestry.umt.edu/ntsg/

Jarvis PG, Leverenz JW (1983) Productivity of temperate deciduous and evergreen forests. In: *Ecosystem Processes: Mineral Cycling, Productivity, and Man's Influence* (eds Lange OL *et al*.), pp. 233–280. Springer-Verlag, New York.

Kato T, Tang YH, Gu S *et al*. (2004a) Carbon dioxide exchange between the atmosphere and an alpine meadow ecosystem on the Qinghai–Tibetan Plateau, China. *Agricultural and Forest Meteorology*, **124**, 121–134.

Kato T, Tang YH, Gu S *et al*. (2004b) Seasonal patterns of gross primary production and ecosystem respiration in an alpine meadow ecosystem on the Qinghai–Tibetan Plateau. *Journal of Geophysical Research – Atmospheres*, **109**, D12109, doi: 12110.11029/12003JD003951.

Kato T, Tang YH, Gu S *et al*. (2006) Temperature and biomass influences on interannual changes in CO_2 exchange in an alpine meadow on the Qinghai–Tibetan Plateau. *Global Change Biology*, **12**, 1285–1298.

Lagergren F, Eklundh L, Grelle A *et al*. (2005) Net primary production and light use efficiency in a mixed coniferous forest in Sweden. *Plant, Cell and Environment*, **28**, 412–423.

Law BE, Falge E, Gu L *et al*. (2002) Environmental controls over carbon dioxide and water vapor exchange of terrestrial vegetation. *Agricultural and Forest Meteorology*, **113**, 97–120.

Leuning R (2004) Measurements of trace gas fluxes in the atmosphere using eddy covariance: WPL corrections revisited. In: *Handbook of Micrometeorology: A Guide for Surface Flux Measurements and Analysis* (eds Lee X *et al*.), pp. 119–132. Kluwer Academic Publishers, Dordrecht, the Netherlands.

Leuning R, Cleugh HA, Zegelin SJ *et al*. (2005) Carbon and water fluxes over a temperate Eucalyptus forest and a tropical wet/dry savanna in Australia: measurements and comparison with MODIS remote sensing estimates. *Agricultural and Forest Meteorology*, **129**, 151–173.

Liu JY, Liu ML, Tian HQ *et al*. (2005) Spatial and temporal patterns of China's cropland during 1990–2000: an analysis based on landsat TM data. *Remote Sensing of Environment*, **98**, 442–456.

Lloyd J, Taylor JA (1994) On the temperature-dependence of soil respiration. *Functional Ecology*, **8**, 315–323.

Running SW, Baldocchi DD, Turner DP (2000) Global terrestrial gross and net primary productivity from the earth observation system. In: *Methods in Ecosystem Science* (eds Sala OE *et al*.), pp. 31–34. Springer-Verlag, New York.

Running SW, Baldocchi DD, Turner DP *et al*. (1999) A global terrestrial monitoring network integrating tower fluxes, flask sampling, ecosystem modeling and EOS satellite data. *Remote Sensing of Environment*, **70**, 108–127.

Running SW, Nemani RR, Heinsch FA *et al*. (2004) A continuous satellite-derived measure of global terrestrial primary production. *Bioscience*, **54**, 547–560.

Turner DP, Ritts WD, Cohen WB *et al*. (2003) Scaling gross primary production (GPP) over boreal and deciduous forest landscapes in support of MODIS GPP product validation. *Remote Sensing of Environment*, **88**, 256–270.

Turner DP, Ritts WD, Cohen WB *et al*. (2005) Site-level evaluation of satellite-based global terrestrial gross primary production and net primary production monitoring. *Global Change Biology*, **11**, 666–684.

Webb EK, Pearman GI, Leuning R (1980) Correction of flux measurements for density effects due to heat and water vapor transport. *Quarterly Journal of the Royal Meteorological Society*, **106**, 85–100.

Wen XF, Yu GR, Sun XM *et al*. (2006) Soil moisture effect on the temperature dependence of ecosystem respiration in a subtropical Pinus plantation of southeastern China. *Agricultural and Forest Meteorology*, **137**, 166–175.

Willmott CJ (1982) Some comments on the evaluation of model performance. *Bulletin of the American Meteorological Society*, **63**, 1309–1313.

Yu GR, Wen XF, Sun XM *et al*. (2006) Overview of Chinaflux and evaluation of its eddy covariance measurement. *Agricultural and Forest Meteorology*, **137**, 125–137.

Zhang YQ, Shen YJ, Yu Q *et al*. (2002) Variation fluxes of water vapor, sensible heat and carbon dioxide above winter wheat and maize canopies. *Journal of Geographical Sciences*, **12**, 295–300.

Zhang YQ, Tang YH (2005) Inclusion of photoinhibition in simulation of carbon dynamics of an alpine meadow on the Qinghai-Tibetan Plateau. *Journal of Geophysical Research-Biogeosciences*, **110**, G01007, doi: 10.1029/2005JG000021.

Zhang YQ, Tang YH, Jiang J, Yang YH (2007) Characterizing the dynamics of soil organic carbon in grasslands on the Qinghai-Tibetan Plateau. *Science in China (Series D)*, **50**, 113–120.

Zhang YQ, Wegehenkel M (2006) Integration of MODIS data into a simple model for the spatial distributed simulation of soil water content and evapotranspiration. *Remote Sensing of Environment*, **104**, 393–408.

Zhang YQ, Yu Q, Liu CM *et al*. (2005) Simulation of CO_2 and latent heat fluxes in the North China Plain. *Science In China Series D-Earth Sciences*, **48**, 172–181.

